13th International Conference on Greenhouse Gas Control Technologies, GHGT-13, 14-18 November 2016, Lausanne, Switzerland

Development of Cost Effective and High Performance Composite for CO_2 Capture in Ca-Cu Looping Process

Saima Sultana Kazi[a], Asunción Aranda[a], Luca di Felice[a], Julien Meyer[a],*

Ramón Murillo[b], Gemma Grasa[b]

[a]Institute for Energy Technology (IFE), Department of Environmental Technology, Instituttveien 18, 2007, Kjeller, Norway
[b]Instituto de Carboquímica (ICB-CSIC),C/Miguel Luesma Castán 4, 50018, Zaragoza, Spain

Abstract

New cost effective and high performance bi-functional composite materials consisting of CaO and CuO supported on $Ca_{12}Al_{14}O_{33}$ have been developed for the calcium-copper (Ca-Cu) looping process. A hydrothermal method has been used to synthesize the materials from low cost precursors. Prepared composites are characterised by X-ray diffraction, scanning electron microscopy together with energy-dispersive spectroscopy mapping, and by crushing strength tests. Long term chemical performances of the materials are tested in a thermo-gravimetric analyser. The composite containing 53 wt% CuO, 22 wt% CaO and 25 wt% $Ca_{12}Al_{14}O_{33}$ shows stable CO_2 capture (~15 g-CO_2/100g composite) and O_2 carrying capacity (~7 g-O_2/100g composite) in long term Ca-Cu multi-cycle, and shows satisfactory mechanical strength compared to reference materials used in the Ca-Cu process.

1. Introduction

Fossil fuel combustion is the major contributor for increasing CO_2 concentration in the atmosphere which

---

* Corresponding author. Tel.: +47-99-46-08-95
  E-mail address: julien.meyer@ife.no

consequently leads to global warming. CO_2 capture and storage technology (CCS) is claimed to have the potential to reduce these CO_2 emissions by producing concentrated CO_2 streams from fossil fuel power plants or industry intensive industries ready for transportation to safe storage sites. The three main approaches to capture CO_2 are post- and pre-combustion capture, as well as oxy-fuel combustion. The most common pre-combustion process uses steam reforming with amine scrubbing as CO_2 capture technology to produce H_2 from natural gas [1]. An alternative approach for H_2 production from hydrocarbons is the sorption enhanced reforming (SER) process with *in-situ* removal of CO_2 by means of CaO-based high temperature sorbent. The key advantages of SER are: (i) Overall process simplification and intensification, (ii) lower reforming reaction temperature and (iii) higher hydrogen yield (95 to 99 mol %, dry basis) compared to conventional steam reforming [2, 3].

Recently, a cost effective and energy efficient calcium-copper looping (Ca-Cu) process has been proposed by Abanades *et al.* for hydrogen production with CO_2 capture [4, 5]. The Ca-Cu process is a hybrid between the SER process (combining reforming and a $CaO/CaCO_3$ cycle for high temperature CO_2 capture) and the chemical looping process (where a metal oxide provides O_2 and heat in the reduction reaction of the fuel). This coupling allows a gaseous fuel to be oxidized in a N_2 free environment, avoiding the use of an expensive air separation unit (ASU) for oxy-fuel combustion of the fuel [6-8], and shows potential for lower capture cost [9-12]. In this integrated process, two endothermic-exothermic reaction pairs are matched in the same reactor. The energy needed to drive the endothermic reforming reaction is provided by the heat produced *in-situ* from the carbonation reaction of the CaO-based sorbent. Similarly, the energy required for the calcination of $CaCO_3$ is matched with the one produced *in-situ* by the reduction of the metal oxide, i.e. CuO.

In the Ca-Cu process, the chemical and thermal performance of the materials over cycles is the key to achieve high energy and CO_2 capture efficiencies at reasonable cost. The decrease in performance of Ca-Cu looping materials is due to the presence of CuO (melting point, 1358 K) which makes it vulnerable at high temperature. De Diego *et al.* [13] and Qin *et al.* [14] showed that the oxygen carrying capacity of pure CuO decreases rapidly with repeated oxidation/reduction cycles due to agglomeration of CuO. Therefore, CuO needs to be combined with an inert support to avoid agglomeration. The inert support (e.g. Al_2O_3, $Ca_{12}Al_{14}O_{33}$) enhances (1) the reactivity of CaO and CuO, (2) the mechanical strength, and (3) attrition resistance [9, 13]. Separate particles of CaO and CuO can be employed in the Ca-Cu looping process [5] to minimize the effect of CuO agglomeration on the reversibility of the sorbent. On the other hand, composite particles of CaO and CuO have the advantage of transferring heat efficiently for the endothermic calcination of $CaCO_3$. Moreover, composite materials can reduce the overall amount of inert support in the materials, potentially reducing their cost [15]. Several efforts have been made to develop a single composite for Ca-Cu looping to enhance the cyclic stability of CaO/CuO [4, 14, 16]. Anthony *et al.* [17] designed a core-in-shell CaO/CuO composite to provide heat for the regeneration of $CaCO_3$. Qin *et al.* [18] studied the behaviour of CaO/CuO based composite in a combined Ca-Cu looping process. Kierzkowska *et al.* [10] developed Cu-functionalized CaO based sorbents using a co-precipitation method. All the results reported a decrease in CO_2 capture and O_2 carrying capacity in cyclic carbonation/calcination and oxidation/reduction cycles, respectively. Therefore, more efforts are necessary to enhance the performance of CaO-CuO composites for use in the Ca-Cu looping process.

The objective of the present work was to develop a cost effective and high performance CaO-CuO composite material by optimizing the total inert fraction of the solids. For this purpose, a recently developed simple and cost effective synthesis method [19] to produce $CaO/Ca_{12}Al_{14}O_{33}$ sorbent from low cost precursors, based on the decomposition of hydrogarnet ($Ca_3Al_2(OH)_{12}$), has been adapted to produce CaO-CuO composites.

2. Experimental

2.1. Synthesis of bi-functional CaO-CuO composite materials

Bi-functional CaO-CuO based composite materials with different mayenite ($Ca_{12}Al_{14}O_{33}$) inert contents (15 wt%, 20 wt% and 25 wt %) were synthesized by hydrothermal method using $Ca(OH)_2$ (Emsure, 96 %), AlOOH (Sasol, 95 %), and CuO (Alfa Aesar, 99.9 %) as the precursors. The CuO content in the prepared composites was 50-60 wt% and the molar ratio of CuO/CaO equal to 2. Stoichiometric amounts of the precursors were weighed and mixed together in isopropanol using a magnetic stirrer to obtain homogeneous slurry. Isopropanol was evaporated at 383 K

overnight. After evaporation of the isopropanol, the dried powders were transferred to a 600 cm^3 stainless steel autoclave. Deionized water was added to the powder at a liquid to solid weight ratio equal to 3. The slurry was heated to 423 K for 5 h in closed autoclave for hydrothermal synthesis. After completion of the hydrothermal reaction, the product from the autoclave was cooled down and dried in a heating cabinet at 383 K. The dried powders were calcined in air at 1273 K for 1 h (heating rate, 10 K.min^{-1}) to obtain the final composite material.

2.2. Preparation of composite particles by pelletization

CaO-CuO composite powders produced from hydrothermal synthesis were pelletized using a uniaxial press (50 MPa). The pellets were calcined in air at 1273 K for 1 h. Finally, the calcined pellets were crushed and sieved to the desired particle size (0.8 mm < dp < 1 mm).

2.3. Preparation of composite particles by high shear agglomeration

Agglomerates of CaO-CuO composite particles were prepared using a high shear wet granulator (GMX-LAB Micro, Vector Corporation). Before agglomeration, hydrothermally synthesized CaO-CuO composite powders were carbonated at 923 K in 100 vol% CO_2 in a tube furnace to avoid stickiness to the granulator bowl (prevent formation of $Ca(OH)_2$).

About 70 g of the carbonated composite powders were loaded into the high shear granulator bowl. The impeller and chopper speeds were adjusted to 1500 and 3600 rpm, respectively. The composite powders were pre-mixed for 5 min. A 15 wt% polyethylene glycol (PEG 4000) binder solution was added through the peristaltic pump to the powder until the agglomerates formed. The measured torque value from the impeller was used to control the agglomeration process. After completion of the agglomeration process, the particles were dried at 383 K overnight. Dried particles were then calcined in air at 1273 K for 1 h to remove the organic binder and to partially sinter the granulated composite material. Finally, the granulated calcined composites were sieved to the size fraction of 0.8 mm < dp < 1 mm.

2.4. Preparation of epoxy embedded composite particles

A mixture of resin (Epofix) and hardener (Epofix) was prepared with a ratio of 15 and 2 parts by volume. The mixture was stirred gently with a rod so that no air was entrapped into the solution. The prepared mixture was then poured over few composite particles kept in the mould and solidified at room temperature. The epoxy-embedded specimen was polished with abrasive papers of 500, 800, 1000 (silicon carbide, SiC) until a smooth surface of the particles appears. Finally, the surface was polished with a diamond paste.

2.5. Characterization of composites

The constituent phases of the CaO-CuO composite materials were identified by X-ray diffraction (XRD), using a Bruker D8 advanced diffractometer equipment with CuKα radiation (λ = 1.5406 Å, with 40 kV and 40 mA). The XRD diffractograms were obtained in the angular range of 10-90° using step-size 0.02° and the scan time per step was 2 seconds. The cross-section of selected composite particles was studied by Scanning Electron Microscopy (SEM), (Hitachi S-4800N), with Energy-Dispersive Spectroscopy (EDS) mapping. Prior to imaging, composite particles embedded in epoxy were sputter-coated with carbon to inhibit charging of the particles. To evaluate the mechanical strength of the composite particles, the crushing strength was measured using a manually operated digital force gauge (Shimpo, FGV-10X).

The material compositions and their names corresponding to the components and weight percentages are given in Table 1.

Table 1. Compositions and names of the prepared CaO-CuO-$Ca_{12}Al_{14}O_{33}$ composites.

Material composition	Name
61 wt% CuO/ 24 wt% CaO/ 15 wt% $Ca_{12}Al_{14}O_{33}$	Cu61- Ca24- CA15
57 wt% CuO/ 23 wt% CaO/ 20 wt% $Ca_{12}Al_{14}O_{33}$	Cu57- Ca23- CA20
53 wt% CuO/ 22 wt% CaO/ 25 wt% $Ca_{12}Al_{14}O_{33}$	Cu53- Ca22- CA25

2.6. Performance of the bi-functional composites over multiple Ca-Cu looping cycles

The cyclic CO_2 capture and O_2 carrying capacity of the CaO-CuO composite materials were evaluated using a thermo-gravimetric analyser (**TGA, CI electronics**).

A small amount (~ 40 mg, size fraction, 0.8 < dp < 1mm) of calcined material was placed in an alumina crucible and heated up to 1143 K at a rate of 9 K.min^{-1} under 100 vol% N_2. The following cycle describes the main steps of the Ca-Cu looping process, i.e. reforming/carbonation, oxidation, reduction/calcination. When the temperature reaches 1143 K, reduction was performed in an atmosphere containing 60 vol% CO_2, 20 vol% H_2 and 20 vol% H_2O. After a reduction time of 2 min, temperature was lowered to 923 K in 70 vol% N_2, 25 vol% H_2O and 5 vol% H_2. Carbonation, simulating the reforming step in the Ca-Cu process, was performed at 923 K in 15 vol% CO_2, 25 vol% H_2O and 60 vol% N_2 for 25 min. After the carbonation, temperature was increased again to 1143 K in 90 vol% CO_2 and 10 vol% H_2O. Oxidation was then performed at 1143 K for 20 min in an atmosphere containing 75 vol% CO_2 and 25 vol% air to re-oxidise Cu to CuO. In the next step, calcination of $CaCO_3$ in presence of 40 vol% CO_2, 25 vol% H_2O, and 35 vol% N_2 was performed. For all composites, carbonation/calcination and oxidation/reduction cycles were repeated over 40 cycles to determine the long term behaviour of the composites. The cyclic CO_2 capture capacity (g-CO_2/100g composite) and O_2 carrying capacity (g-O_2/100g composite) are calculated from the weight changes during carbonation/calcination and oxidation/reduction as a function of time. The multi-cycle steps and testing conditions are summarized in Table 2.

Table 2. Steps and testing conditions of Ca-Cu looping process in TGA (Total gas flow, F_{total} = 500 cm^3/min).

Reduction	Cooling	Carbonation	Heating	Oxidation	Calcination
1143K, 2min	1143K to 923K	923K, 25 min	923K to 1143K	1143K, 20min	1143K, 15min
60 vol% CO_2	70 vol% N_2	15 vol% CO_2	90 vol% CO_2	75 vol% CO_2	40 vol% CO_2
20 vol% H_2	25 vol% H_2O	25 vol% H_2O	10 vol% H_2O	25 vol% air	25 vol% H_2O
20vol% H_2O	5 vol% H_2	60 vol% N_2			35 vol% N_2

3. Results and discussions

Fig.1 shows that XRD diffractograms of the composites after calcination at 1273 K for 1 h. All composites exhibit three different constituent phases, tenorite (CuO), calcium oxide (CaO) and mayenite ($Ca_{12}Al_{14}O_{33}$). These phases are confirmed by their characteristic main peaks, CuO (2θ = 35.8, 39.1, 49.30, 61.78, 68.45), CaO (2θ = 32.51, 37.50, 54.21, 79.92) and $Ca_{12}Al_{14}O_{33}$ (2θ = 18.23, 33.34, 41.33, 55.15 and 57.55), respectively.
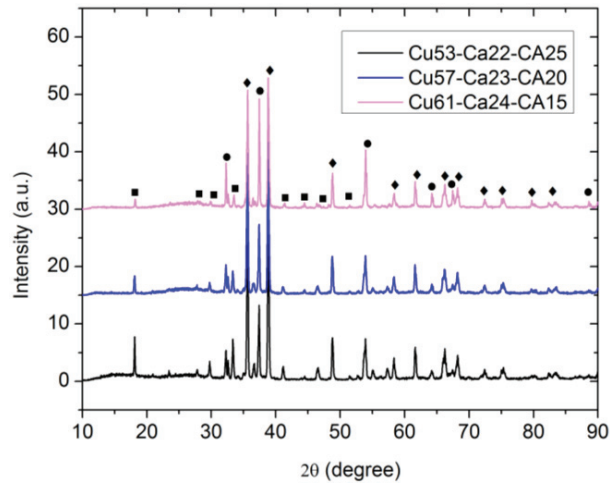
Fig. 1. X-ray diffraction patterns of the prepared composites after calcination in air at 1273 K for 1 h; Phases: (●) CaO; (♦) CuO; (■) $Ca_{12}Al_{14}O_{33}$.

The CO_2 capture and the O_2 carrying capacity of the three composite materials (pelletized and agglomerated) in long term carbonation/calcination and oxidation/reduction multi-cycles are plotted in Figs. 2, 3 and 4. Fig. 2a and 2b show the CO_2 capture and O_2 carrying capacity of the agglomerated composite Cu61-Ca24-CA15. The composite loses half of its CO_2 capture capacity after 15 cycles and stabilizes at ~10 g-CO_2/100g composite after 42 cycles. The O_2 carrying capacity of the material decreases linearly with the number of cycles and attains 4.2 g-O_2/100g composite after 42 cycles (Fig. 2b).
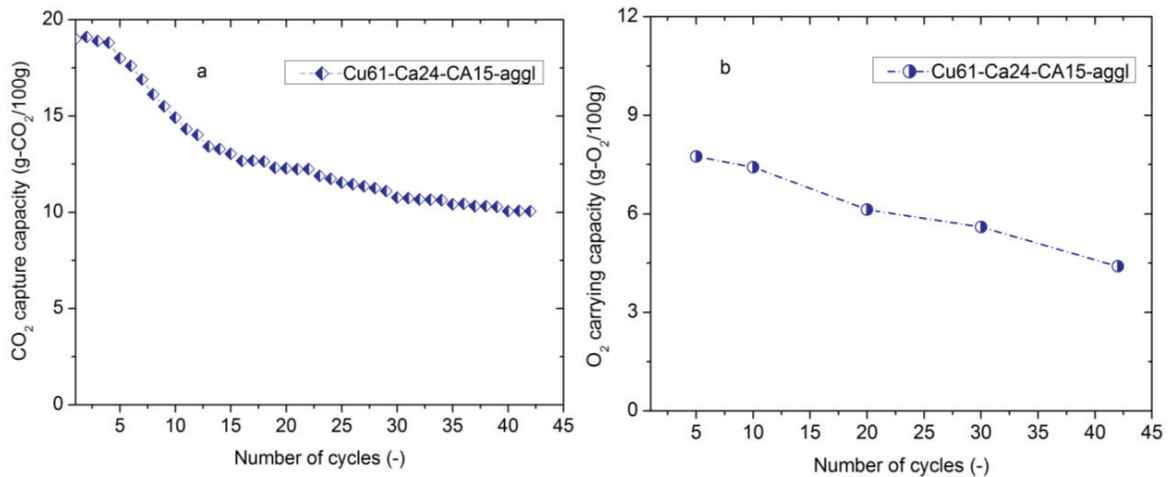

Fig. 2. (a) CO_2 capture and (b) O_2 carrying capacity of CaO-CuO composite (Cu61-Ca24-CA15) over 42 cycles in TGA; Carbonation temperature is 923 K; Calcination/oxidation/reduction temperature is 1143 K.

The composite material Cu57-Ca23-CA20 (pelletized and agglomerated) shows a maximum CO_2 capture capacity of 18 g-CO_2/100g composite for the 1st cycle, declining slowly to reach 15.5 g-CO_2/100g composite after 44 cycles, but without reaching stabilization (Fig. 3a). The pelletized and agglomerated composites show approximately the same behaviour. On the other hand, Fig. 3b shows that the initial O_2 carrying capacity (~10 g-O_2/100g composite) of the composite (pelletized and agglomerated) declines rapidly and stabilizes at ~5.3 g-O_2/100g composite after 30 cycles.
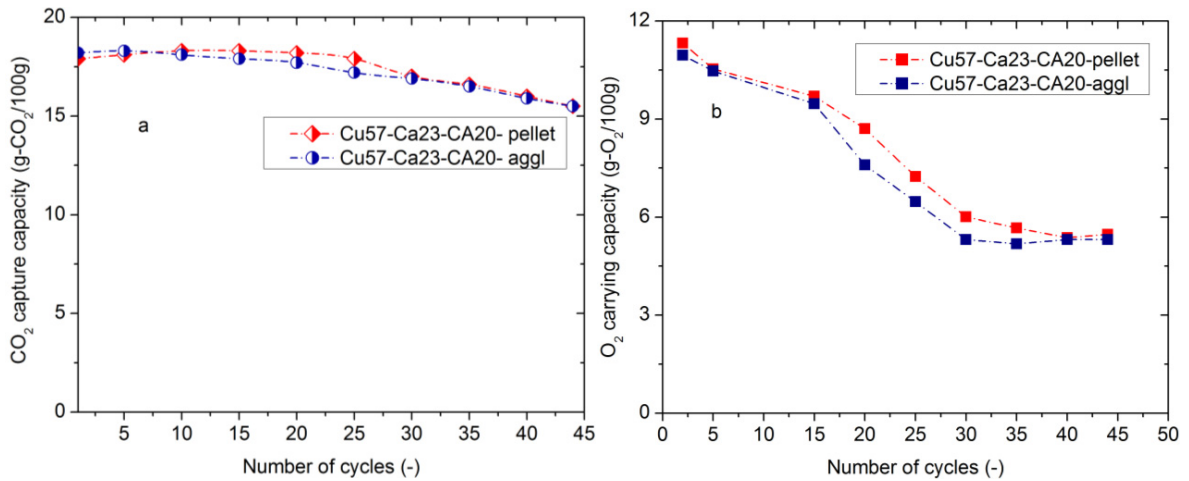
Fig. 3. (a) CO_2 capture and (b) O_2 carrying capacity of CaO-CuO composite (Cu57-Ca23-CA20) over 44 cycles in TGA; Carbonation temperature is 923 K; Calcination/oxidation/reduction temperature is 1143 K.

Stabilisation of both CO_2 capture and O_2 carrying capacity is observed for the Cu53-Ca22-CA25 composite (pelletized and agglomerated). The initial CO_2 capture capacity of ~16 g-CO_2/100g composite stabilizes to ~15 g-CO_2/100g composite after 50 cycles for both the pelletized and agglomerated composites (Fig. 4a). Fig. 4b shows that the O_2 carrying capacities of both materials decrease from ~ 9.7 g-O_2/100g composite to reach a stable value of ~ 7.3 g-O_2/100g composite after 50 cycles.
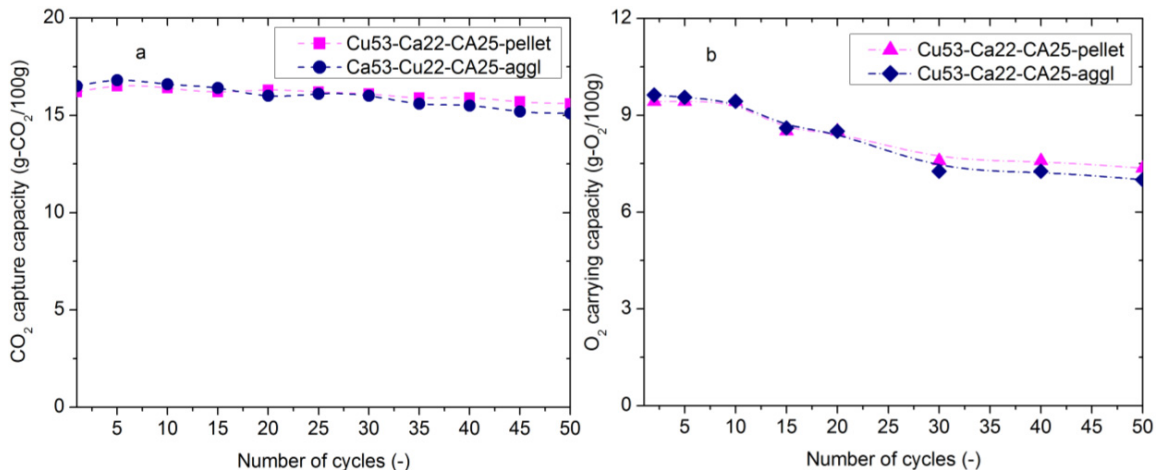

Fig. 4. (a) CO_2 capture and (b) O_2 carrying capacity of CaO-CuO based composite (Cu53-Ca22-CA25) over 50 cycles in TGA; Carbonation temperature is 923 K; Calcination/oxidation/reduction temperature is 1143 K.

The results from TGA multi-cycle tests for the prepared composite materials are summarized in Table 3. It can be observed that the CO_2 capture and O_2 carrying capacity of the prepared composites decreases in the multi-cycle runs. This could be due to the substantial changes in distribution of Cu/CuO on the surface of CaO within the composites [14]. The loss in CO_2 capture and O_2 carrying capacity is more pronounced for the Cu61-Ca24-CA15 composite. The high percentage of CuO in the composite may then deteriorate the reactivity of CaO (for CO_2 capture) due to the sintering of Cu/CuO at high temperature [17]. In order to prevent the sintering of CaO and CuO, the $Ca_{12}Al_{14}O_{33}$ inert support is introduced in the prepared composites [19-21]. The multi-cycle tests show that an increased amount of inert support reduces the sintering of CaO and hence maintains a stable CO_2 capture capacity, a

better stability is obtained for Cu57-Ca23-CA20 and Cu53-Ca22-CA25 composites. Among the prepared composites, Cu53-Ca22-CA25 containing 53 wt% CuO, 22 wt% CaO and 25 wt% of $Ca_{12}Al_{14}O_{33}$ shows the best stability performance for the Ca-Cu looping process conditions tested.

Table 3. Summary of theoretical and experimental CO_2 capture and O_2 carrying capacity of the synthesized composites before and after TGA multi-cycles.

Composite	Ratio CuO/CaO	CO_2 capture capacity (g-CO_2/100g composite)			O_2 carrying capacity (g-O_2/100g composite)		
		Theoretical	Experimental		Theoretical	Experimental	
			1st cyc	last cyc		1st cyc	last cyc
Cu61-Ca23-CA15 (aggl.)	2	19.0	19.0	10.0	12.2	9.5	4.2
Cu57-Ca23-CA20 (pellet)	2	18.0	17.9	15.8	11.4	10.2	5.4
Cu57-Ca23-CA20 (aggl.)	2	18.0	18.0	15.5	11.4	9.9	5.3
Cu53-Ca22-CA25 (pellet)	2	17.0	16.2	15.5	10.6	9.6	7.5
Cu53-Ca22-CA25 (aggl.)	2	17.0	16.5	15.1	10.6	9.8	7.2

To assess the decrease in CO_2 capture and O_2 carrying capacity of the composite materials in multi-cycle tests, a cross sectional study with SEM/EDS mapping has been performed for material (Cu53-Ca22-CA25) before and after test.
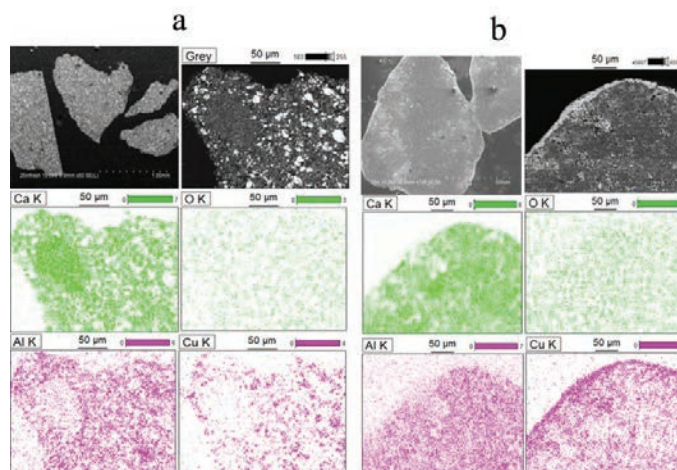

Fig. 5. SEM/EDS mapping of cross section images of the composite Cu53-Ca22-CA25; (a) fresh (before cycling) and (b) used (after cycling) EDS mappings show the distribution of different elements in the composite before and after cycling, respectively.

SEM micrographs and their corresponding EDS mapping (Fig. 5a) of the fresh sample show that the composite particles are well separated and Cu particles (bright part) are almost homogeneously distributed all over the composites. On the other hand, SEM/EDS mapping of the same composite after long term TGA cycling (50 cycles) shows that constituent particles are connected to each other due to sintering (Fig. 5b).

Fig. 5a and 5b clearly show that Cu/CuO has migrated towards the surface of the composite and agglomerated to form a thin layer after multi-cycling. This thin layer wraps over the CaO grains, and hinders partially the diffusion of CO_2. The development of this Cu/CuO layer seems to stabilize with successive cycles and results in a stable CO_2 capture and O_2 carrying capacity when the CuO content is reduced and the sintering is moderate.

Mechanical strength is related to the particle's composition and to the preparation method. Mechanical properties of the composite particles have been evaluated by measuring their crushing strength. Crushing strength of the composite particles was measured on 100 particles with a particle size between 0.8 and 1 mm. The median crushing strength of the prepared composites is summarized in Table 4. As expected, the composite Cu53-Ca22-CA25

containing 25 wt% $Ca_{12}Al_{14}O_{33}$ inert support shows the best crushing strength (11 N). The crushing strength has also been measured for a calcined limestone and a commercial reforming catalyst as reference materials.

Table 4. Crushing strength measurements on three different $CuO-CaO-Ca_{12}Al_{14}O_{33}$ composites and reference materials

Material	Preparation method	Median crushing strength, (N)
Cu61-Ca24-CA15	Aggl. with 15 wt% PEG, calcined 1273K, 1h	6.1
Cu57-Ca23-CA20	Aggl. with 15 wt% PEG, calcined 1273K, 1h	6.0
Cu53-Ca22-CA25	Aggl. with 15 wt% PEG, calcined 1273K, 1h	11.0
Rheinkalk limestone	Calcined 1073K, 2h	9.0
Commercial reforming catalyst		27.0

4. Conclusions

A hydrothermal preparation method was used to synthesize from low cost precursors CaO-CuO composites supported on a mayenite ($Ca_{12}Al_{14}O_{33}$) inert. The best results have been obtained for the composite material containing 53 wt% CuO, 22 wt% CaO and 25 wt% $Ca_{12}Al_{14}O_{33}$, and show a stable CO_2 capture and O_2 carrying capacity of ~15 g-CO_2/100g and ~7 g-O_2/100g respectively in a simulated Ca-Cu looping multi-cycle. The observed migration and agglomeration of Cu/CuO on the surface of the particles reduce the CO_2 capture and O_2 carrying capacity. However, this effect can be minimized by reducing the CuO loading. A crushing strength of 11N has been obtained for this material, showing satisfactory mechanical stability compared to reference materials used in the Ca-Cu process. This new bi-functional CaO-CuO composite material may reduce the material costs of the Ca-Cu looping process due to the reduction of the overall inert material content.

Acknowledgements

References

[1] J.R. Rostrup-Nielsen, Steam reforming, in: Handbook of Heterogeneous Catalysis, Wiley-VCH Verlag GmbH & Co. KGaA, 2008.
[2] D.P. Harrison, Calcium enhanced hydrogen production with CO_2 capture, Energy Procedia, 1 (2009) 675-681.
[3] K. Johnsen, H.J. Ryu, J.R. Grace, C.J. Lim, Sorption-enhanced steam reforming of methane in a fluidized bed reactor with dolomite as CO_2-acceptor, Chemical Engineering Science 61 (2006) 1195-1202.
[4] J.C. Abanades, R. Murillo, J.R. Fernandez, G. Grasa, I. Martínez, New CO_2 capture process for hydrogen production combining Ca and Cu chemical loops, Environmental Science & Technology, 44 (2010) 6901-6904.
[5] J.R. Fernández, J.C. Abanades, R. Murillo, G. Grasa, Conceptual design of a hydrogen production process from natural gas with CO_2 capture using a Ca–Cu chemical loop, International Journal of Greenhouse Gas Control, 6 (2012) 126-141.
[6] J. Blamey, E.J. Anthony, J. Wang, P.S. Fennell, The calcium looping cycle for large-scale CO_2 capture, Progress in Energy and Combustion Science, 36 (2010) 260-279.
[7] D.Y. Lu, R.W. Hughes, E.J. Anthony, Ca-based sorbent looping combustion for CO_2 capture in pilot-scale dual fluidized beds, Fuel Processing Technology, 89 (2008) 1386-1395.
[8] L.M. Romeo, J.C. Abanades, J.M. Escosa, J. Paño, A. Giménez, A. Sánchez-Biezma, J.C. Ballesteros, Oxyfuel carbonation/calcination cycle for low cost CO_2 capture in existing power plants, Energy Conversion and Management, 49 (2008) 2809-2814.
[9] M. Ishida, H. Jin, A novel combustor based on chemical-looping reactions and its reaction kinetics, Journal of Chemical Engineering of Japan, 27 (1994) 296-301.
[10] Q. Imtiaz, A.M. Kierzkowska, C.R. Müller, Coprecipitated, copper-based, alumina-stabilized materials for carbon dioxide capture by chemical looping combustion, ChemSusChem, 5 (2012) 1610-1618.

[11] J. Gale, H. Herzog, J. Braitsch, R. Kuusik, A. Trikkel, A. Lyngfelt, T. Mattisson, Greenhouse Gas Control Technologies 9, High temperature behavior of NiO-based oxygen carriers for chemical looping combustion, Energy Procedia, 1 (2009) 3885-3892.

[12] P. Cho, T. Mattisson, A. Lyngfelt, Comparison of iron-, nickel-, copper- and manganese-based oxygen carriers for chemical-looping combustion, Fuel, 83 (2004) 1215-1225.

[13] L.F. de Diego, P. Gayán, F. García-Labiano, J. Celaya, A. Abad, J. Adánez, Impregnated CuO/Al_2O_3 oxygen carriers for chemical-looping combustion: avoiding fluidized bed agglomeration, Energy & Fuels, 19 (2005) 1850-1856.

[14] C. Qin, J. Yin, W. Liu, H. An, B. Feng, Behavior of CaO/CuO based composite in a combined calcium and copper chemical looping process, Industrial & Engineering Chemistry Research, 51 (2012) 12274-12281.

[15] J. Adánez, P. Gayán, J. Celaya, L.F. de Diego, F. García-Labiano, A. Abad, Chemical looping combustion in a 10 kWth prototype using a CuO/Al_2O_3 oxygen carrier: Effect of operating conditions on methane combustion, Industrial & Engineering Chemistry Research, 45 (2006) 6075-6080.

[16] V. Manovic, E.J. Anthony, Integration of calcium and chemical looping combustion using composite CaO/CuO-based materials, Environmental Science & Technology, 45 (2011) 10750-10756.

[17] V. Manovic, Y. Wu, I. He, E.J. Anthony, Core-in-shell CaO/CuO-based composite for CO_2 capture, Industrial & Engineering Chemistry Research, 50 (2011) 12384-12391.

[18] C. Qin, J. Yin, C. Luo, H. An, W. Liu, B. Feng, Enhancing the performance of CaO/CuO based composite for CO_2 capture in a combined Ca–Cu chemical looping process, Chemical Engineering Journal, 228 (2013) 75-86.

[19] S.S. Kazi, A. Aranda, J. Meyer, J. Mastin, 12th International Conference on Greenhouse Gas Control Technologies, GHGT-12, High performance CaO-based sorbents for pre- and post- combustion CO_2 capture at high temperature, Energy Procedia, 63 (2014) 2207-2215.

[20] J. Mastin, A. Aranda, J. Meyer, 10th International Conference on Greenhouse Gas Control Technologies, New synthesis method for CaO-based synthetic sorbents with enhanced properties for high-temperature CO_2 -capture, Energy Procedia, 4 (2011) 1184-1191.

[21] Z.-s. Li, N.-s. Cai, Y.-y. Huang, Effect of preparation temperature on cyclic CO_2 capture and multiple carbonation−calcination cycles for a new Ca-based CO_2 sorbent, Industrial & Engineering Chemistry Research, 45 (2006) 1911-1917.